This article has been accepted for publication in a future issue of this journal, but has not been fully edited. Content may change prior to final publication. Citation information: DOI 10.1109/JESTPE.2017.2724847, IEEE Journal of Emerging and Selected Topics in Power Electronics



# Development of an Improved Tri-State Buck-Boost Converter with Optimized Type-3 Controller

Niraj Rana, *Student Member, IEEE,* Arnab Ghosh, *Member, IEEE* and Subrata Banerjee, *Senior Member, IEEE*

***Abstract*—In this paper, design & development of Tri-state Buck-Boost converter with particle swarm optimization (PSO) based optimized Type-3 controller is discussed. In conventional Buck-Boost converter a right-half-plane (RHP) zero is present in its control-to-output transfer function. So, it becomes difficult to design controller for the converter which is operating in continuous conduction mode (CCM). Converter performance deteriorates due to the presence of RHP zero in its control-to-output transfer function. The proposed Tri-state Buck-Boost converter has no RHP zero in its control-to-output transfer function. In closed-loop control, PSO based optimized Type-3 controller has been designed and utilized to improve the transient and steady-state performances. Simulation and experimental results of proposed converter have been presented and compared with conventional Buck-Boost converter. The proposed converter exhibit faster transient and steady-state characteristic and it can be used wherever fast transient response with step-up/step-down of source voltage is needed and also be useful for drive applications, electric vehicles and photovoltaic system etc. In this work, PSO based optimized Type-3 control technique is newly introduced to enhance the closed-loop performance of Tri-state Buck-Boost converter and not been reported earlier in any literature. The closed-loop converter is very cheap and easily implantable due to use of simple control logic by utilizing few analog components.**

***Index Terms*—Buck-Boost converter, non-minimum phase system, Tri-state Buck-Boost converter, small-signal modeling, optimized Type-3 controller.**

## I. Introduction

CONVENTIONAL Buck-Boost DC-DC switch mode power converter (SMPC) is a popular power electronics device for step-up/step-down the source voltage [1]. Buck-Boost converter is applicable when source voltage fluctuates in certain ranges, e.g. power factor correction (PFC) circuit, photovoltaic system etc. It can be employed with Maximum Power Point Tracking (MPPT) system for efficient & reliable solar power generation. For applications like as MPPT, PFC and drives system, DC-DC SMPC should be efficient and reliable. It should also possess good transient and steady-state characteristics regardless to load and source disturbances. But in conventional Buck-Boost converter has non-minimum phase problem due to the presence of a right-half-plane (RHP) zero in its control-to-output transfer function when converter operate in Continuous Conduction Mode (CCM). It is observed that presence of a RHP zero in its control-to-output transfer function deteriorates the converter performances. Any system having an open-loop RHP zero can be identified by its initial counter response (undershoot) of output voltage to a step input voltage [2]. The effect due to RHP zero in conventional Buck-Boost converter in time domain can be explained as, an initial dip (undershoot) in output voltage results in control system triggering an increase in the duty cycle ratio, which causes an increased output filter capacitor discharging time. This result in the output voltage dipping even further until the inductor current builds up to recharge the filter capacitor [3]. It becomes more severe when operating point is changed because RHP zero moves in complex s-plane. Therefore, designers don't get the freedom to increase the bandwidth beyond certain limits which is limited by the worst case RHP zero location and it generally restricts the bandwidth to $1/30^{th}$ of the switching frequency [4].

There are some techniques proposed earlier in literatures for removal of RHP zero in SMPC. Some techniques are reported in [5] which can reduce the effect of RHP zero in SMPC: (i) Reducing inductor size can't eliminate the RHP zero but moves it farther towards the right half plane, so the RHP zero effect will be reduced on the system response. But, it causes higher inductor current ripple and hence increased conduction and switching losses (ii) decreasing the switching frequency increases the inductor current ripple as well as increases output voltage ripple and hence requires large size output filter capacitor (iii) DCM operation can remove the RHP zero but increases inductor current ripple. Hence overall efficiency will be decreased. Output voltage ripple of SMPC can remove the RHP zero effect if the equivalent series resistance (ESR) of output filter capacitor is sufficiently large as proposed in [6] by "leading-edge-modulation" method. Tri-state topology technique has been discussed [7]-[9] for completely removal of RHP zero from converter plant without going for DCM

N. Rana is with the Department of Electrical Engineering, National Institute of Technology Durgapur, Durgapur-713209, India (e-mail: nirajranaosme@gmail.com).

A. Ghosh is with the Department of Electrical Engineering, Dr. B. C. Roy Engineering College Durgapur, Durgapur-713206, India (e-mail: aghosh.ee@gmail.com).

S. Banerjee is with the Department of Electrical Engineering, National Institute of Technology Durgapur, Durgapur-713209, India (e-mail: bansub2004@yahoo.com).

This article has been accepted for publication in a future issue of this journal, but has not been fully edited. Content may change prior to final publication. Citation information: DOI 10.1109/JESTPE.2017.2724847, IEEE Journal of Emerging and Selected Topics in Power Electronics



operation by introducing an additional degree of control choice. It has been established that proposed Tri-state Buck-Boost converter is superior to other RHP zero removal methods.

This type of Tri-state converter has an additional mode of operation in the form of inductor freewheeling mode in CCM operation that results completely removal of RHP zero from control-to-output transfer function from switching converter. Thus, there is no such problem of non-minimum phase in Tri-state type of converter and the closed-loop dynamic performances of the converter can be improved. The main contribution of this work is to develop an improved Tri-state Buck-Boost converter with optimized Type-3 controller which can be used in applications wherever fast-response buck/boost action is needed. The proposed topology of Tri-state Buck-Boost converter (Fig.1) is simple and different from the existing topology ([8], [13]) which is basically cascade connection of Buck and Boost converters for single-phase power factor correction. The small-signal model for Tri-state Buck-Boost converter has been developed by using state-space averaging technique [10]-[14]. It has been observed that the proposed converter has no RHP zero in its control-to-output transfer function.

For closed-loop control Type-3 controller has been designed and utilized for better performance and stability. Initially, Type-3 controller has been designed by using "*K-factor*" approach [15]-[18] and its transfer function has been optimized by using PSO based optimization technique [19]-[21] to improve the transient and steady-state characteristics of the proposed converter. PSO technique is based on the behaviour of biologically living things, like as "swarm of insects", "birds flocking" and "fish schooling". The insects, animals, birds, fish etc. always travel in a group without crashing each other from their group members by adjusting their positions and velocities from using their group information [22]. Some prior work has already been published in the field of DC-DC switching converters by utilizing optimized controller [23]-[36]. Here, PSO based optimized Type-3 control technique is newly introduced to enhance the closed-loop performance of Tri-state Buck-Boost converter and not been reported earlier in any literature. Simulation and experimental results of proposed Tri-state Buck-Boost converter & conventional Buck-Boost converter have been presented and a comparative study has been done. The results clearly demonstrate the superior transient and steady-state performances of the proposed Tri-state Buck-Boost converter with PSO based optimized Type-3 controller. The cost of proposed converter is very less and it is easily implantable due to use of simple control logic by utilizing few analog components.

The proposed Tri-state converter can be used in applications wherever fast-response buck/boost action is needed. Any fast-response SMPS to provide power for (i) new generation DSP/Microprocessor systems (ii) electronic goods and gadgets (iii) telecom power supplies (iv) critical medical equipment/instruments etc., one can use Tri-state Buck-Boost or Tri-state Flyback (isolated type) converter. DC-DC converters derived from Tri-state topology having high bandwidth may be suitable for some specific applications like (i) process control plant and robot automated factories (ii) automotive industries (iii) space power distribution systems (iv) hybrid vehicles. For maximum power extraction from solar photo voltaic (SPV) panels, use of such converters may be beneficial due to its fast transient response.

## II. TRI-STATE BUCK-BOOST CONVERTER

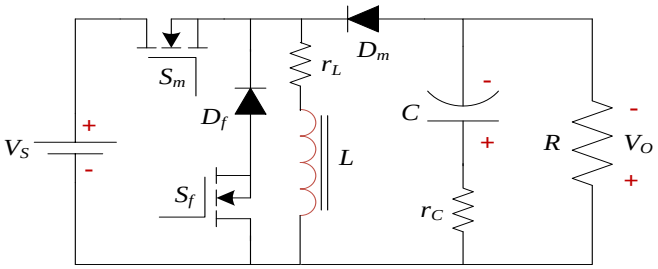


Fig.1. Power circuit of Tri-state Buck-Boost converter.

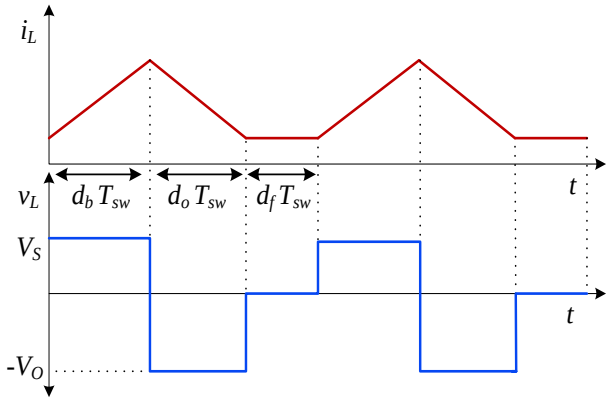


Fig.2. Steady-state waveforms of inductor current ($i_L$) and inductor voltage ($v_L$) of Tri-state Buck-Boost converter.

The power circuit of proposed Tri-state Buck-Boost converter is shown in Fig.1. Here $V_S$ is the DC input voltage, $L$ is the inductor, $S_m$ and $D_m$ are the main switch and main diode, $S_f$ and $D_f$ are the freewheeling switch and freewheeling diode across the inductor, $C$ is the output filter capacitor, $r_L$ and $r_C$ are the ESR (Equivalent Series Resistance) of inductor and capacitor and $R$ is the load resistance. The proposed converter under steady state has three modes of operation. (i) *'Buck-Boost'* mode ($d_bT_{sw}$). Here, $d_b$ is the duty ratio for this mode and $T_{sw}$ is the switching period of the converter. In the *'buck-boost'* mode, $S_m$ is *on*, $S_f$ is *off* and the inductor current increases due to the source voltage. The diode $D_m$ is reverse biased and capacitor $C$ maintain the load voltage. (ii) *'Capacitor-Charging'* mode ($d_oT_{sw}$). Here, $d_o$ is the duty ratio for this mode. In the *'capacitor-charging'* mode both switches ($S_m$ and $S_f$) are in off condition, the diode $D_m$ is forward biased and the inductor current decreases as the power transfer to the load, with the capacitor $C$ being charged. (iii) *'Freewheeling'* mode ($d_fT_{sw}$). Here, $d_f$ is the duty ratio for this mode. In the *'Freewheeling'* mode $S_m$ is *off*, $S_f$ is *on* and the inductor current is in the freewheeling state. Once again the diode $D_m$ is reverse biased and the capacitor $C$ maintain the load voltage. After combining these three modes, it can be written as,

This article has been accepted for publication in a future issue of this journal, but has not been fully edited. Content may change prior to final publication. Citation information: DOI 10.1109/JESTPE.2017.2724847, IEEE Journal of Emerging and Selected Topics in Power Electronics



$$d_b + d_o + d_f = 1 \quad (1)$$

Fig.2 shows the steady-state waveform of inductor current ($i_L$) and inductor voltage ($v_L$) in CCM operation where the inductor current flows continuously [$i_L(t)>0$]. Since in steady-state the time integral of the inductor voltage ($v_L$) over one complete time period must be zero and assuming all the components are ideal, the DC gain of the Tri-state Buck-Boost converter can be written as,

$$V_S \times d_b T_{sw} - V_o \times d_o T_{sw} + 0 \times d_f T_{sw} = 0$$

$$\frac{V_O}{V_S} = \frac{d_b}{d_o} \quad (2)$$

where, $V_S$ is the DC input voltage, $V_O$ is the output voltage. From (2), it is clear that, the output voltage of the converter can be varied by varying the ratio of $d_b/d_o$. If $d_b>d_o$ then converter will operate in boost mode and if $d_b<d_o$ then converter will operate in buck mode.

Assuming a loss-less converter, $P_{in} = P_o$

Therefore, $V_S I_S = V_o I_o$

and $$\frac{V_O}{V_S} = \frac{I_S}{I_O} = \frac{d_b}{d_o} \quad (3)$$

where, $P_{in}$ is the input power, $P_O$ is the output power, $I_S$ is the source current and $I_O$ is the load current.

It is to be noted that efficiency of the proposed Tri-state Buck-Boost converter becomes less compared to conventional Buck-Boost converter due to the losses incurred in the additional circuit elements (*i.e.* use of one extra MOSFET & one Diode as shown in Fig.1).

## III. Small-Signal Modeling of Tri-state Buck-Boost Converter

The DC-DC converters are highly nonlinear time-varying system. The state-space averaging technique is an approximation technique that approximates the converter as a continuous linear system [14]. The state-space modeling of Tri-state Buck-Boost converter is described below. The converter has three modes of operation under steady-state. The state variables are considered as inductor current ($i_L$) and capacitor voltage ($v_C$). The state equations of Tri-state Buck-Boost converter in matrix form during different modes are given below,

### A. Mode-I: - Buck-Boost mode ($d_bT_{sw}$)

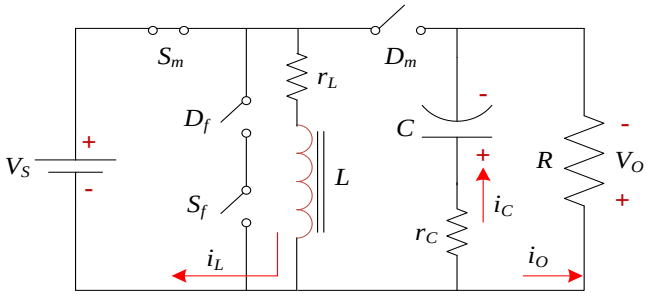


Fig.3. Equivalent circuit of converter during Mode-I.

The equivalent circuit of the proposed converter during Mode-I ($d_bT_{sw}$) operation is shown in Fig.3. Here switch $S_m$ is *on*, switch $S_f$ is *off* and both diodes $D_m$ & $D_f$ are *off*. The state-space equation in matrix form is given below in (4).

$$\begin{bmatrix} \frac{di_L}{dt} \\ \frac{dv_C}{dt} \end{bmatrix} = \begin{bmatrix} \frac{-r_L}{L} & 0 \\ 0 & \frac{-1}{C(R+r_C)} \end{bmatrix} \begin{bmatrix} i_L \\ v_C \end{bmatrix} + \begin{bmatrix} \frac{1}{L} \\ 0 \end{bmatrix} V_S \quad (4)$$

### B. Mode-II: - Capacitor-Charging mode ($d_oT_{sw}$)

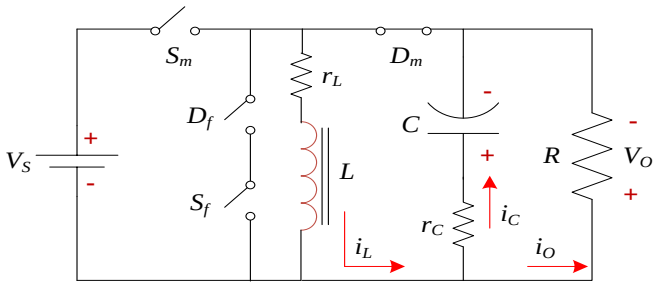


Fig.4. Equivalent circuit of converter during Mode-II.

Similarly, the equivalent circuit of the proposed converter during Mode-II ($d_oT_{sw}$) operation is shown in Fig.4, where both switches $S_m$ & $S_f$ are *off* condition, diode $D_m$ is *on* condition and diode $D_f$ is *off* condition. The state-space equation in matrix form is given below in (5).

$$\begin{bmatrix} \frac{di_L}{dt} \\ \frac{dv_C}{dt} \end{bmatrix} = \begin{bmatrix} \frac{-(r_L R + r_L r_C + r_C R)}{L(R+r_C)} & \frac{-R}{L(R+r_C)} \\ \frac{R}{C(R+r_C)} & \frac{-1}{C(R+r_C)} \end{bmatrix} \begin{bmatrix} i_L \\ v_C \end{bmatrix} \quad (5)$$

### C. Mode-III: - Freewheeling mode ($d_fT_{sw}$)

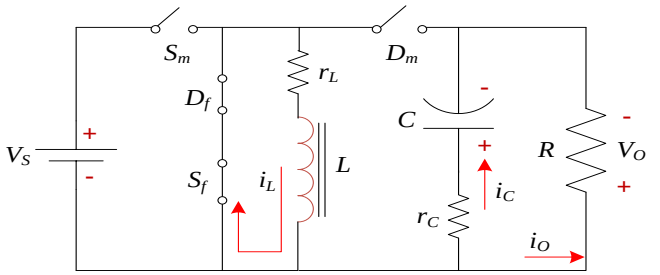


Fig.5. Equivalent circuit of converter during Mode-III.

The equivalent circuit of the converter during Mode-III ($d_fT_{sw}$) operation is shown in Fig.5. In this mode switch $S_f$ and diode $D_f$ are *on* condition, switch $S_m$ and diode $D_m$ are *off* condition. The state-space equation in matrix form is given below in (6).

$$\begin{bmatrix} \frac{di_L}{dt} \\ \frac{dv_C}{dt} \end{bmatrix} = \begin{bmatrix} \frac{-r_L}{L} & 0 \\ 0 & \frac{-1}{C(R+r_C)} \end{bmatrix} \begin{bmatrix} i_L \\ v_C \end{bmatrix} \quad (6)$$

The state-space average equation over one complete switching period of the converter can be written as,

This article has been accepted for publication in a future issue of this journal, but has not been fully edited. Content may change prior to final publication. Citation information: DOI 10.1109/JESTPE.2017.2724847, IEEE Journal of Emerging and Selected Topics in Power Electronics



$$\begin{bmatrix} \frac{di_L}{dt} \\ \frac{dv_C}{dt} \end{bmatrix} = \begin{bmatrix} \frac{-(r_L R + r_L r_C + d_o r_C R)}{L(R+r_C)} & \frac{-d_o R}{L(R+r_C)} \\ \frac{d_o R}{C(R+r_C)} & \frac{-1}{C(R+r_C)} \end{bmatrix} \begin{bmatrix} i_L \\ v_C \end{bmatrix} + \begin{bmatrix} \frac{d_b}{L} \\ 0 \end{bmatrix} V_S \quad (7)$$

$$\Rightarrow \frac{di_L}{dt} = \left( \frac{-(r_L R + r_L r_C + d_o r_C R)}{L(R+r_C)} \right) i_L + \left( \frac{-d_o R}{L(R+r_C)} \right) v_C + \frac{d_b}{L} V_S \quad (8)$$

$$\Rightarrow \frac{dv_C}{dt} = \left( \frac{d_o R}{C(R+r_C)} \right) i_L + \left( \frac{-1}{C(R+r_C)} \right) v_C \quad (9)$$

Now, for obtaining the converter control-to-output transfer function, introducing small ac perturbations in (8) & (9) and separate them into ac and dc components and applying the Laplace transformation to convert all the ac terms into s-domain.

Let us consider the perturbed variables are, $i_L = I_L + \tilde{i}_L$, $v_C = V_C + \tilde{v}_C$, $v_O = V_O + \tilde{v}_O$ and $d_b = D_b + \tilde{D}_b$, Here, $d_o = D_o$ is keeping constant.

$$\frac{d}{dt}(I_L + \tilde{i}_L) = \left( \frac{-(r_L R + r_L r_C + D_o r_C R)}{L(R+r_C)} \right)(I_L + \tilde{i}_L) + \left( \frac{-D_o R}{L(R+r_C)} \right)(V_C + \tilde{v}_C) + \frac{(D_b + \tilde{D}_b)}{L} V_S \quad (10)$$

$$\frac{d}{dt}(V_C + \tilde{v}_C) = \left( \frac{D_o R}{C(R+r_C)} \right)(I_L + \tilde{i}_L) + \left( \frac{-1}{C(R+r_C)} \right)(V_C + \tilde{v}_C) \quad (11)$$

Now, separating ac and dc components in (10) & (11) and can be written as,

$$\frac{d}{dt}(\tilde{i}_L) = \left( \frac{-(r_L R + r_L r_C + D_o r_C R)}{L(R+r_C)} \right)(\tilde{i}_L) + \left( \frac{-D_o R}{L(R+r_C)} \right)(\tilde{v}_C) + \frac{V_S}{L}(\tilde{D}_b) \quad (12)$$

and

$$\left( \frac{-(r_L R + r_L r_C + D_o r_C R)}{L(R+r_C)} \right)(I_L) + \left( \frac{-D_o R}{L(R+r_C)} \right)(V_C) + \frac{(D_b)}{L} V_S = 0 \quad (13)$$

$$\frac{d}{dt}(\tilde{v}_C) = \left( \frac{D_o R}{C(R+r_C)} \right)(\tilde{i}_L) + \left( \frac{-1}{C(R+r_C)} \right)(\tilde{v}_C) \quad (14)$$

$$\text{and} \left( \frac{D_o R}{C(R+r_C)} \right)(I_L) + \left( \frac{-1}{C(R+r_C)} \right)(V_C) = 0 \quad (15)$$

Now, taking Laplace Transform of (12) and (14) and neglecting the steady-state equations.

$$sI_L(s) = \left( \frac{-(r_L R + r_L r_C + D_o r_C R)}{L(R+r_C)} \right) I_L(s) + \left( \frac{-D_o R}{L(R+r_C)} \right) V_C(s) + \frac{V_S}{L} D_b(s) \quad (16)$$

$$sV_C(s) = \left( \frac{D_o R}{C(R+r_C)} \right) I_L(s) + \left( \frac{-1}{C(R+r_C)} \right) V_C(s) \quad (17)$$

Therefore, the control-to-capacitor voltage transfer function of Tri-state Buck-Boost converter can be obtained from (16) and (17).

$$\frac{V_C(s)}{D_b(s)} = \frac{V_S}{L} \times \frac{1}{s^2 \frac{C(R+r_C)}{RD_O} + s \frac{(1 - MC(R+r_C))}{RD_O} + \left( N - \frac{M}{RD_O} \right)} \quad (18)$$

where, $M = \frac{-(r_L R + r_L r_C + D_O r_C R)}{L(R+r_C)}$ and $N = \frac{RD_O}{L(R+r_C)}$

The relation between the capacitor voltage and output voltage of the converter can be written as,

$$v_O = r_C i_C + v_C \quad (19)$$

$$v_O = r_C C \frac{dv_C}{dt} + v_C \quad (20)$$

Now, introducing small ac perturbations in (20) and separate them into ac and dc components and applying the Laplace transformation to convert all the ac terms into *s*-domain.

$$V_O + \tilde{v}_O = r_C C \frac{d}{dt}(V_C + \tilde{v}_C) + (V_C + \tilde{v}_C) \quad (21)$$

Now, taking Laplace Transform of (21) and neglecting the steady-state equation.

$$V_C(s) = \frac{V_O(s)}{(1 + s r_C C)} \quad (22)$$

Now, putting the value of $V_C(s)$ from (22) into (18), the final control-to-output transfer function of the Tri-state Buck-Boost converter can be written as,

$$T_{Tri\_buck\_boost}(s) = \frac{V_O(s)}{D_b(s)} = \frac{V_S}{L} \times \frac{(1 + s r_C C)}{s^2 \frac{C(R+r_C)}{RD_O} + s \frac{(1 - MC(R+r_C))}{RD_O} + \left( N - \frac{M}{RD_O} \right)} \quad (23)$$

From the above equation (23), it is clear that the RHP zero is absent in the transfer function of the Tri-state Buck-Boost converter, but a LHP zero is present due to the ESR of the capacitor. In case of conventional Buck-Boost converter a RHP zero is present in its control-to-output transfer function (24) [11].

$$T_{buck\_boost}(s) = \frac{V_O(s)}{D(s)} = G_{do} \times \frac{(1 + s/\omega_{z-ESR})(1 - s/\omega_{z-RHP})}{\left( s^2/\omega_O^2 + s/(\omega_O Q) + 1 \right)} \quad (24)$$

where, $D$ is the duty cycle ratio of conventional Buck-Boost converter.

$$G_{do} \simeq \frac{V_S}{(1-D)^2}, \omega_{z-ESR} = \frac{1}{r_C C} rad/s,$$

$$\omega_{z-RHP} = \frac{(1-D)^2 R}{DL} rad/s, \omega_O \simeq \frac{(1-D)}{\sqrt{LC}} rad/s$$

and Quality Factor, $Q = R(1-D)\sqrt{\frac{C}{L}}$

From (24), it is clear that a RHP zero has present in the transfer function of the conventional Buck-Boost converter.

This article has been accepted for publication in a future issue of this journal, but has not been fully edited. Content may change prior to final publication. Citation information: DOI 10.1109/JESTPE.2017.2724847, IEEE Journal of Emerging and Selected Topics in Power Electronics



TABLE I
Parameter Valuesof Converters

| Sl. No. | Parameter | Design Value |
|---|---|---|
| 1 | Source Voltage $V_S$ | 6-20 V |
| 2 | Output Voltage $V_O$ | 20-6 V |
| 3 | Inductor $L$ | 275 µH |
| 4 | ESR of inductor $r_L$ | 0.3 Ω |
| 5 | Output Filter Capacitor $C$ | 540 µF |
| 6 | ESR of Capacitor $r_C$ | 0.2 Ω |
| 7 | Load Resistance $R$ | 30-60 Ω |
| 8 | Switching frequency $f_{sw}$ | 20 kHz |
| 9 | Switching Period $T_{sw}$ | 50µs |
| 10 | Constant Duty Ratio $D_O$ | 0.2 |

After putting the above parameter values from Table I in (23) and (24), the transfer function of Tri-state Buck-Boost converter and conventional Buck-Boost converter are obtained and given below in (25) and (26),

$$T_{Tri\_buck\_boost}(s)=\frac{1435.4(s+9259)}{(s+895.3)(s+461)} \tag{25}$$

$$T_{buck-boost}(s)=\frac{-0.6152(s-8182)(s+2500)}{(s+2102)(s+253.1)} \tag{26}$$

## IV. Type-3 Controller

The design of controller plays an important role for achieving desired closed-loop performance of the converter. The controller can also help to shape the open loop transfer function to achieve the overall system stability and fastest transient response. The Type-3 controller is a cascaded two lead controllers with a pole at origin. So, this type of controller can provide maximum 180° "*phase-boost*" with zero steady-state error [18]. The pole at the origin provides a very high gain at low frequencies and the pole-zero pairs reduce the phase shift between the frequency of the two zeros and the frequency of two poles as lead controller. So, this controller may provide 0° to 180° phase boost with zero steady-state error. The Type-3 controller is intended for switching converters that exhibit a –40 dB/decade roll-off above the poles of the output filter and a –180° phase lag. This extends the loop bandwidth. Type-3 controller network can achieve a very fast dynamic response and they are commonly used for systems requiring very fast transient response.

### A. Op-Amp based Type-3 controller

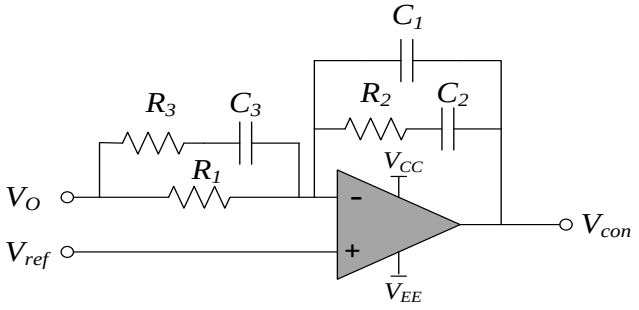


Fig.6. Circuit diagram of Type-3 controller

An analog Op-Amp based Type-3 controller is shown in Fig.6, where six passive circuit components are required. The control voltage ($V_{con}$) to the output voltage ($V_O$) transfer function of the controller in Fig.6 can be written as,

$$T_{Type-3}(s)=\frac{V_{con}(s)}{V_O(s)}=\frac{(1+sC_2R_2)\left[1+sC_3(R_1+R_3)\right]}{sR_1(C_1+C_2)(1+sC_3R_3)(1+sC_{12}R_2)} \tag{27}$$

where, $C_{12}=\dfrac{C_1C_2}{C_1+C_2}$, parallel connection of two capacitors $C_1$ and $C_2$.

### B. Mathematical Approach

The generalized transfer function of Type-3 controller is given below,

$$T_{Type-3}(s)=\frac{(1+s/\omega_{z1-T3})(1+s/\omega_{z2-T3})}{(s/\omega_{p0-T3})(1+s/\omega_{p1-T3})(1+s/\omega_{p2-T3})} \tag{28}$$

Now, comparing (27) and (28), getting the values of poles & zeros in terms of passive circuit components (resistor & capacitor).

$$f_{z1-T3}=\frac{1}{2\pi C_2R_2};\ f_{z2-T3}=\frac{1}{2\pi C_3(R_1+R_3)};\ f_{p1-T3}=\frac{1}{2\pi C_3R_3};$$

$$f_{p2-T3}=\frac{1}{2\pi C_{12}R_2}\ \text{ and }\ f_{p0-T3}=\frac{1}{2\pi R_1(C_1+C_2)}$$

The Type-3 controller having one pole ($f_{p0\text{-}T3}$) at origin and two high frequency poles ($f_{p1\text{-}T3}$ & $f_{p2\text{-}T3}$) are considered at same point. Similarly two zeros ($f_{z1\text{-}T3}$ & $f_{z2\text{-}T3}$) are assumed at same point. So, the double pole and double zero have been located at $\omega_{z1\text{-}T3}=\omega_{z2\text{-}T3}=\omega_{z1,2\text{-}T3}$ and $\omega_{p1\text{-}T3}=\omega_{p2\text{-}T3}=\omega_{p1,2\text{-}T3}$.

$$T_{Type-3}(s)=\frac{(1+s/\omega_{z1,2-T3})^2}{(s/\omega_{p0-T3})(1+s/\omega_{p1,2-T3})^2} \tag{29}$$

The magnitude of the controller can be written as,

$$\left|T_{Type-3}(j\omega)\right|=\frac{\left|1+j\dfrac{\omega}{\omega_{z1,2-T3}}\right|\left|1+j\dfrac{\omega}{\omega_{z1,2-T3}}\right|}{\left|j\dfrac{\omega}{\omega_{p0-T3}}\right|\left|1+j\dfrac{\omega}{\omega_{p1,2-T3}}\right|\left|1+j\dfrac{\omega}{\omega_{p1,2-T3}}\right|} \tag{30}$$

The argument of the controller can be written as,

$$\phi\left(T_{Type-3}(j\omega)\right)=2\tan^{-1}\left(\frac{\omega}{\omega_{z1,2-T3}}\right)-2\tan^{-1}\left(\frac{\omega}{\omega_{p1,2-T3}}\right)-\frac{\pi}{2} \tag{31}$$

The Bode diagram of Type-3 controller is shown in Fig.7. Type-3 controller can provide maximum 180° "*phase-boost*" by varying the location of pole & zero. Here the pole & zero combinations produce a "*phase-boost*" of 160° at a certain frequency. The frequency where maximum "*phase-boost*" can be obtained by taking the derivate of (31) with respect to frequency '$f$' [16].

$$\frac{d}{df}\phi\left(T_{Type-3}(j\omega)\right)=\frac{d}{df}\left(2\tan^{-1}\left(\frac{f}{f_{z1,2-T3}}\right)-2\tan^{-1}\left(\frac{f}{f_{p1,2-T3}}\right)\right) \tag{32}$$

$$or,\ \frac{2}{f_{z-T3}\left(\dfrac{f^2}{f_{z1,2-T3}^2}+1\right)}-\frac{2}{f_{p-T3}\left(\dfrac{f^2}{f_{p1,2-T3}^2}+1\right)}=0 \tag{33}$$

By solving '$f$' from (33), the maximum "*phase-boost*" can be obtained at the "*geometric mean of the double zero-double pole*" frequencies in the controller and can be written in (34)

This article has been accepted for publication in a future issue of this journal, but has not been fully edited. Content may change prior to final publication. Citation information: DOI 10.1109/JESTPE.2017.2724847, IEEE Journal of Emerging and Selected Topics in Power Electronics



below,

$$f_{\max-T3} = \sqrt{f_{z1,2-T3} \times f_{p1,2-T3}} \tag{34}$$

Therefore, $f_{max\text{-}T3}$ is considered as crossover frequency ($f_{c\text{-}T3}$) of Type-3 controller.

### C. Derivation of "K-factor" for Type-3 Controller

In Type-3 controller "*K-factor*" is the ratio between double pole frequency to the double zero frequency [15]. The relationship between *K* and the "*phase-boost*" can be written as follows,

$$phase-boost = 2\left(\tan^{-1}\sqrt{K} - \tan^{-1}\frac{1}{\sqrt{K}}\right) \tag{35}$$

By solving (35) using trigonometric formula, *K* can be written as,

$$K = \left\{\tan\left(\frac{phase-boost}{4} + \frac{\pi}{4}\right)\right\}^2 \tag{36}$$

Equation (36) is known as "*K-factor*" of Type-3 controller & was introduced by "Dean-Venable".

Thus, the double zero & double pole locations can be obtained as,

$$f_{z1,2-T3} = f_{c-T3}/\sqrt{K} = f_{c-T3}/\tan\{(phase-boost+\pi)/4\} \tag{37}$$

and

$$f_{p1,2-T3} = f_{c-T3}\times\sqrt{K} = f_{c-T3}\times\tan\{(phase-boost+\pi)/4\} \tag{38}$$

The location of the double zero & double pole of the Type-3 controller can be calculated by using (37) & (38) for a particular crossover frequency ($f_{c\text{-}T3}$) and necessary "*phase-boost*" of the controller.

### D. Mid-Band Gain of Type-3 Controller

The controller transfer function of (28) can be written as,

$$T_{Type-3}(s) = \frac{s}{\omega_{z1-T3}} \times \frac{(1+\omega_{z1-T3}/s)(1+s/\omega_{z2-T3})}{(s/\omega_{p0-T3})(1+s/\omega_{p1-T3})(1+s/\omega_{p2-T3})}$$

$$T_{Type-3}(s) = G_{O-T3} \times \frac{(1+\omega_{z1-T3}/s)(1+s/\omega_{z2-T3})}{(1+s/\omega_{p1-T3})(1+s/\omega_{p2-T3})} \tag{39}$$

where, $G_{O\text{-}T3}$ is the Mid-Band Gain of the controller and $G_{O-T3} = \omega_{p0-T3}/\omega_{z1-T3}$. The value of $\omega_{p0-T3}$ depends on the required gain at crossover frequency. $G_{O\text{-}T3}$ can be written as,

$$G_{O-T3} = G_{T3} \times \frac{\sqrt{1+\left(\frac{\omega_{c-T3}}{\omega_{p1-T3}}\right)^2}\sqrt{1+\left(\frac{\omega_{c-T3}}{\omega_{p2-T3}}\right)^2}}{\sqrt{1+\left(\frac{\omega_{z1-T3}}{\omega_{c-T3}}\right)^2}\sqrt{1+\left(\frac{\omega_{c-T3}}{\omega_{z2-T3}}\right)^2}} \tag{40}$$

where, $G_{T3}$ is the gain of the selected crossover frequency $f_{c\text{-}T3}$.

$$\omega_{p0-T3} = G_{T3} \times \frac{\omega_{z1-T3}\sqrt{1+\left(\frac{\omega_{c-T3}}{\omega_{p1-T3}}\right)^2}\sqrt{1+\left(\frac{\omega_{c-T3}}{\omega_{p2-T3}}\right)^2}}{\sqrt{1+\left(\frac{\omega_{z1-T3}}{\omega_{c-T3}}\right)^2}\sqrt{1+\left(\frac{\omega_{c-T3}}{\omega_{z2-T3}}\right)^2}} \tag{41}$$

If double poles & zeros are considered at the same point, the formula becomes,

$$\omega_{p0-T3} = G_{T3} \times \frac{\omega_{z1,2-T3}\left(\omega_{p1,2-T3}^2 + \omega_{c-T3}^2\right)}{\omega_{p1,2-T3}^2\sqrt{1+\left(\frac{\omega_{z1,2-T3}}{\omega_{c-T3}}\right)^2}\sqrt{1+\left(\frac{\omega_{c-T3}}{\omega_{z1,2-T3}}\right)^2}} \tag{42}$$

### E. Design Example of Type-3 Controller

Let's consider the converter has a gain deficit of -12 dB at a 1 kHz selected crossover frequency and necessary "*phase-boost*" is $160^o$. From equation (37) & (38), the location of the double zero & double pole is given below,

The location of double zero is

$$f_{z1,2-T3} = 1000/\tan\left\{\left(160^o + 180^o\right)/4\right\} = 87.49Hz \tag{43}$$

and the double pole location is

$$f_{p1,2-T3} = 1000\times\tan\left\{\left(160^o + 180^o\right)/4\right\} = 11.43KHz \tag{44}$$

The gain $G_{T3}$ at 1 kHz selected crossover frequency must be -12 dB. Thus, the position of the 0-dB crossover pole can be obtained as,

$$f_{p0-T3} = \frac{G_{T3}\times f_{z1,2-T3}\times\left(f_{p1,2-T3}^2 + f_{c-T3}^2\right)}{f_{p1,2-T3}^2\times\sqrt{\left(f_{z1,2-T3}/f_{c-T3}\right)^2+1}\times\sqrt{\left(f_{c-T3}/f_{z1,2-T3}\right)^2+1}}$$
$$= 30.46Hz \tag{45}$$

Therefore, the final transfer function of designed Type-3 controller after fine tuning of the gain is given in (46).

$$T_{Type-3}(s) = \frac{66.291(s+605)^2}{s\left(s+3481s+2.825\times10^6\right)} \tag{46}$$

## V. PSO BASED OPTIMIZED TYPE-3 CONTROLLER

### A. A Brief Overview of PSO Algorithm

In the year 1995, "R.C. Eberhart" & "J. Kennedy" presented a soft computing technique named as PSO (Particle Swarm Optimization) algorithm, which was based on the stochastic optimization method [19]-[22]. PSO algorithm technique is an evolutionary optimization algorithm that optimizes the "continuous-discrete", "linear-nonlinear", "constrained-unconstrained" & "non-differentiable" functions by iterative method to improve the solutions for different parameter values [14]. This technique is based on the behaviour of biologically living things, like as "swarm of insects", "birds flocking" & "fish schooling". The insects, animals, birds, fish etc. always travel in a group without crashing each other from their group members by adjusting their positions and velocities from using their group information [34]. A swarm contains numbers of individual, termed "particles"; they change their own positions over the time. Every particle gives a prospective elucidation to a task. In PSO algorithm technique, particles move around in a multi-dimensional search-space. During the movement of swarm every particle adjusts its own position according to its own experience and the experience of its neighbours, making use of the best position come across by it and its neighbours [21]. This results each particle travel in the direction of the better elucidation zones, while still having the ability to search

This article has been accepted for publication in a future issue of this journal, but has not been fully edited. Content may change prior to final publication. Citation information: DOI 10.1109/JESTPE.2017.2724847, IEEE Journal of Emerging and Selected Topics in Power Electronics



a wide area around the better solution areas. The enactment of every particle is measured by pre-defined "fitness-function or objective-function". This "objective-function" is associated to the problem based solution. The PSO algorithm technique has been presented to be robust, optimize solution & fastest solving of the complex problems. In this work, a PSO based optimized Type-3 controller has also been designed & utilized for better performance of the converter and improved overall system stability.

### *B. Objective Function for PSO Algorithm*

For obtaining the optimized performance of the converter, the objective/fitness function selection with performance criteria is the most vital step for tuning the parameters value of Type-3 controller by applying PSO based optimization technique. The minimum value of this fitness function/objective function corresponds to the optimum set of parameter values. Here, integral time weighted absolute error *i.e.* ITAE is a performance criterion that can provide fastest response with small overshoot. So, ITAE is selected as an objective function/fitness function in this work and can be expressed as,

$$F(t)=\int_0^{\gamma} t\left|e(t)\right|dt \tag{47}$$

where, upper limit of the integration $\gamma$ is the steady-state value.

### *C. Mathematical Formulation for PSO Algorithm*

A brief knowledge about mathematical formulation for PSO algorithm has been presented in this subsection. The position of the $i^{th}$ particle among total number of population $n_p$ can be written as,

$$X_i=\left(X_i^1, X_i^2, X_i^3, X_i^4, \ldots X_i^d, \ldots X_i^n\right), \text{ for } i=1,2,3,\ldots n_p \tag{48}$$

where, $X_i^d$ denotes the position of $i^{th}$ particle in $d^{th}$ dimensional search space and $n$ is the entire number of dimensional search space.

To optimize the transfer function of Type-3 controller five parameters or five dimensional search space is required in $n_p$ particle population vector ( $X_i^1$= gain of the controller, $X_i^2$=zero position ($z_{1\text{-}T3}$), $X_i^3$=zero position($z_{2\text{-}T3}$), $X_i^4$= pole position($p_{1\text{-}T3}$) & $X_i^5$ = pole position($p_{2\text{-}T3}$)).

The rate of the change of position (velocity vector) for $i^{th}$ particle is denoted by,

$$v_i=\left(v_i^1, v_i^2, v_i^3, v_i^4, \ldots v_i^d, \ldots v_i^n\right) \tag{49}$$

Each $i^{th}$ particle preserves a memory of its own earlier best position & represented as personal best position, which can be denoted by "$pbest_i$".

$$pbest_i=\left(pbest_i^1, pbest_i^2, \ldots\ldots pbest_i^d, \ldots\ldots pbest_i^n\right) \tag{50}$$

In a swarm the global best particle position among $i^{th}$ particle position represented as "*gbest*" & can be written as,

$$gbest=\left(gbest^1, gbest^2, \ldots\ldots gbest^d, \ldots\ldots gbest^n\right) \tag{51}$$

The global best positions & each particle earlier best positions are related with the particle velocity vector along each dimensional search space & that velocity vector is then used to calculate a new particle position vector. The adjusted velocity & position of each particle can be calculated by using the present velocity and the distance from "$pbest_i$" to "*gbest*" as given below in (52) & (53). "Kennedy" was first introduced the formulae for velocity & position in PSO algorithm [19], [20].

$$v_i^d(t+1)=v_i^d(t)+C_1*rand_1(\ )*\left(pbest_i^d(t)-X_i^d(t)\right)+C_2*rand_2(\ )*\left(gbest^d(t)-X_i^d(t)\right) \tag{52}$$

$$X_i^d(t+1)=X_i^d(t)+v_i^d(t+1) \tag{53}$$

Here, $C_1$ & $C_2$ are the acceleration rate constant, $rand_1()$ & $rand_2()$ are uniform random numbers in between [0, 1], $t$ is the present iteration number.

Appropriate choice of inertia weight ($w$) in (54) affords equilibrium between global and local observations, so require less number of iteration to find an efficient optimize solution. As initially established, often reduces linearly from 0.9 to 0.4 during a simulation of PSO algorithm. Thus, the inertia weight equation can be written as,

$$w=w_{\max}-\left\{\frac{(w_{\max}-w_{\min})}{t_{\max}}\right\}*t \tag{54}$$

where, $w$ is the inertia weight factor & $t_{max}$ is the maximum number of iteration.

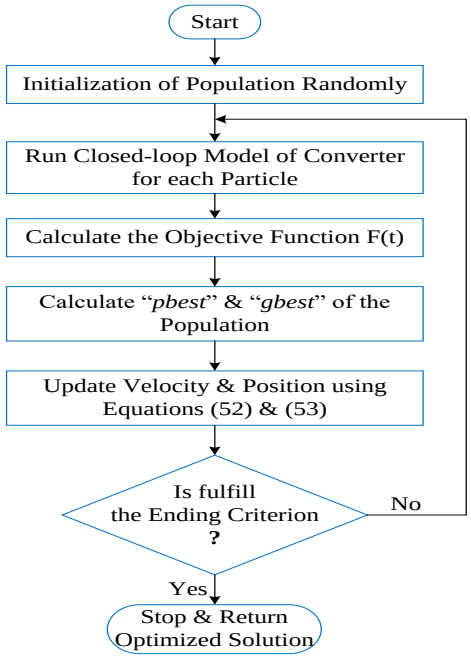


Fig.8. Flowchart for Particle Swarm Optimization (PSO) algorithm.

### *D. Parameters Optimization in PSO based Type-3 Controller*

To obtain optimized Type-3 controller five controller parameters values are to be optimized namely gain of the controller, double zeros ($z_{1,2\text{-}T3}$) and double poles ($p_{1,2\text{-}T3}$). The flowchart for the Particle Swarm Optimization (PSO) algorithm is illustrated in Fig.8. The MATLAB code for PSO algorithm has been written in MATLAB-R2014b. The parameters values for PSO are considered as: (i) Cognitive

This article has been accepted for publication in a future issue of this journal, but has not been fully edited. Content may change prior to final publication. Citation information: DOI 10.1109/JESTPE.2017.2724847, IEEE Journal of Emerging and Selected Topics in Power Electronics



Constant ($C_1$) = 1.5, (ii) Group Constant ($C_2$) = 1.5, (iii) Number of Particles ($n_p$) = 50 & (iv) Maximum number of Iteration ($t_{max}$) = 100. Therefore, the PSO based optimized Type-3 controller transfer function is given below in (55). This Type-3 controller is designed based on Tri-state Buck-Boost converter and also used for closed-loop control of conventional Buck-Boost converter.

$$T_{Type-3}(s) = \frac{973.23(s+586.5)^2}{s(s+3396)^2} \tag{55}$$

## VI. Simulation Results and Discussions

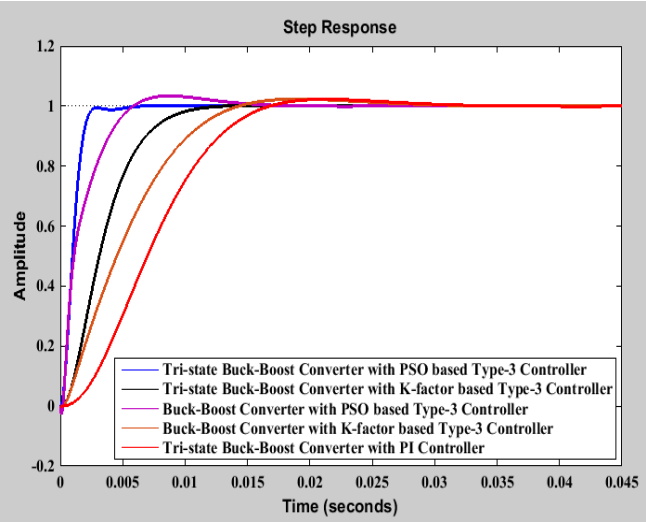


(a)

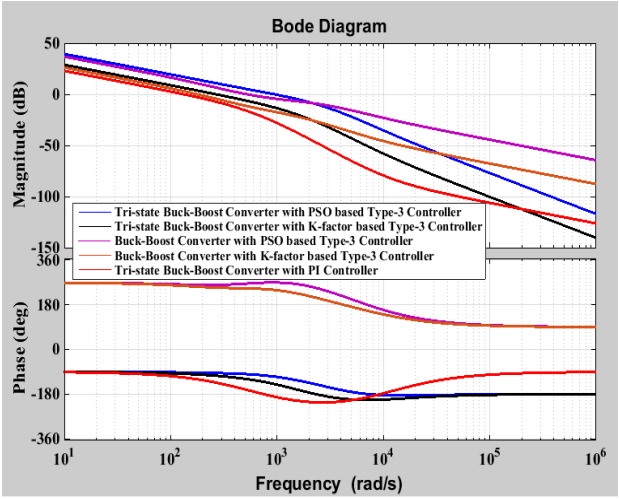


(b)

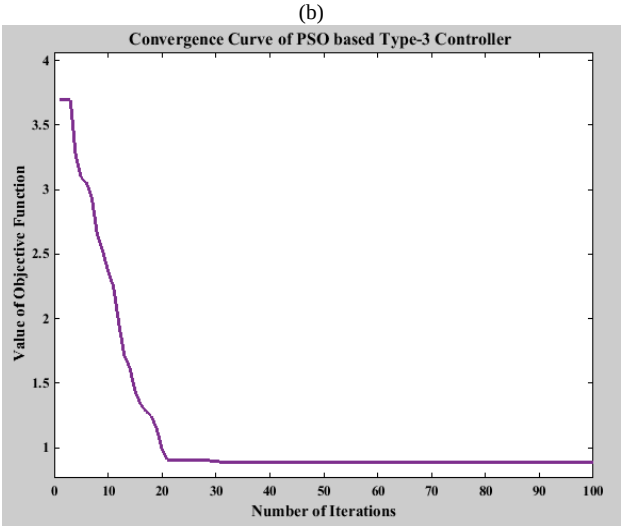


(c)

Fig.9. (a) Step responses (b) Bode Diagram of closed-loop performances of Tri-state Buck-Boost Converter & Conventional Buck-Boost Converter with classical and optimized controllers (c) Convergence curve of objective function ($F(t)$) for PSO based optimized Type-3 controller.

TABLE II
Closed-Loop Performance of the Converters

| Performances | Tri-state Buck-Boost converter with PI controller | Buck-Boost converter with *K-factor* based Type-3 controller | Tri-state Buck-Boost converter with *K-factor* based Type-3 controller | Buck-Boost converter with PSO based Type-3 controller | Tri-state Buck-Boost converter with PSO based Type-3 controller |
|---|---|---|---|---|---|
| Maximum Overshoot($M_P$) | 2.51 % | 2.36 % | 0.159 % | 3.40 % | 0 % |
| Rise Time($t_r$) | 0.01 sec | 0.00904 sec | 0.00574 sec | 0.00354 sec | 0.00147 sec |
| Settling Time ($t_s$) | 0.0237 sec | 0.0219 sec | 0.00983 sec | 0.0121 sec | 0.00239 sec |
| Steady-State Error ($E_{ss}$) | 0 | 0 | 0 | 0 | 0 |
| Gain Margin (*GM*) | 22.3 dB | 22.6 dB | 23.7 dB | 24.5 dB | 28.7 dB |
| Phase Margin (*PM*) | 66.9° | 71.1° | 73.4° | 74° | 75.9° |
| Gain Crossover Frequency (*GCF*) | 133 rad/sec | 648 rad/sec | 767 rad/sec | 521 rad/sec | 946 rad/sec |
| Phase Crossover Frequency (*PCF*) | 744 rad/sec | 5230 rad/sec | 6070 rad/sec | 7080 rad/sec | 7120 rad/sec |
| Controller Transfer Function | $\frac{4.33(7.8\times10^{-5}s+1)}{s}$ | $\frac{66.291(s+605)^2}{s(s+3481s+2.825\times10^6)}$ | $\frac{66.291(s+605)^2}{s(s+3481s+2.825\times10^6)}$ | $\frac{973.23(s+586.5)^2}{s(s+3396)^2}$ | $\frac{973.23(s+586.5)^2}{s(s+3396)^2}$ |
| Closed-loop Stability | Stable | Stable | Stable | Stable | Stable |

The simulation of closed-loop operation of Tri-state Buck-Boost converter and conventional Buck-Boost converter with PSO based optimized Type-3 controller as well as "*K-factor*" based Type-3 controller have been designed and simulated by

This article has been accepted for publication in a future issue of this journal, but has not been fully edited. Content may change prior to final publication. Citation information: DOI 10.1109/JESTPE.2017.2724847, IEEE Journal of Emerging and Selected Topics in Power Electronics



using MATLAB SIMULINK (2014b). The parameters are used for simulation & experimental studies for both the converters are given in Table I. The dynamic performances of both the converters in terms of step response & Bode plot with PSO and "*K-factor*" based Type-3 controller have been observed and shown in Fig.9(a)&(b). Closed-loop performance of Tri-state Buck-Boost converter with PI controller has also been observed and shown in Fig.9(a)&(b). It is observed that Tri-state Buck-Boost converter with PSO based optimized Type-3 controller shows the fastest dynamic response than the conventional Buck-Boost converter. Table II shows the comparative study between Tri-state Buck-Boost converter & conventional Buck-Boost converter. From Table II, it is clear that Tri-state Buck-Boost converter with PSO based optimized Type-3 controller has lesser rise time ($t_r$) & settling time ($t_s$), zero overshoot ($M_P$), zero steady-state error ($E_{ss}$) and higher phase margin ($PM$) in comparison to the conventional Buck-Boost converter. Fig.9(c) shows the convergence curve for PSO based optimized Type-3 controller, which is drawn between values of the Objective function ($F(t)$) vs. number of iterations.

### A. *Dynamic Responses of Output Voltage with Load Resistance Disturbance*

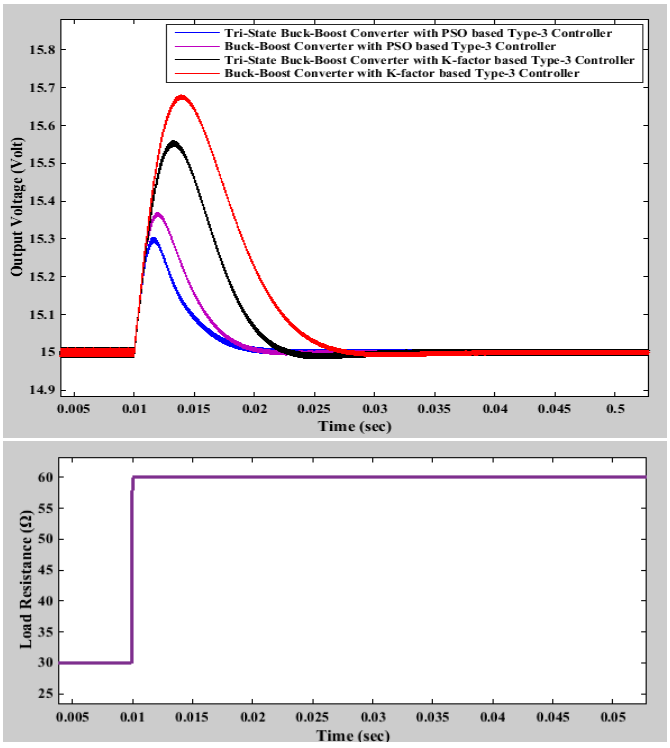


(a)

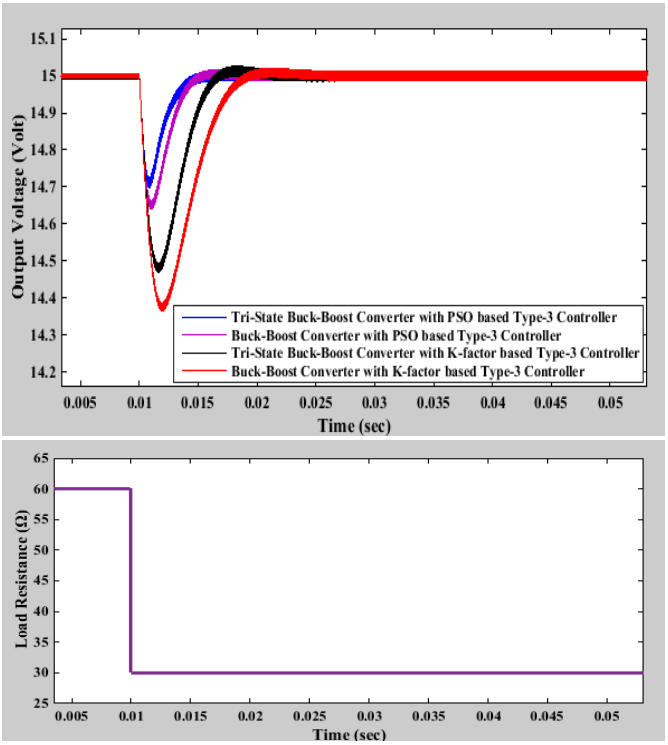


(b)

Fig.10. Dynamic response of output voltage against (a) 50 % step increased and (b) 50 % step decreased of load resistance.

### B. *Tracking Performances of Output Voltage with Reference Voltage Disturbance*

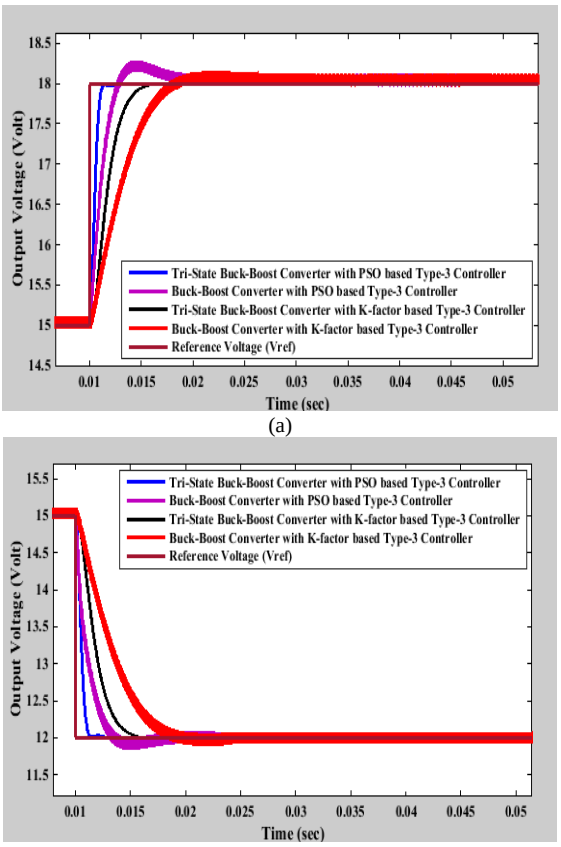


(a)

(b)

Fig.11. Dynamic response of output voltage against (a) 20 % step increased & (b) 20 % step decreased of reference voltage.

This article has been accepted for publication in a future issue of this journal, but has not been fully edited. Content may change prior to final publication. Citation information: DOI 10.1109/JESTPE.2017.2724847, IEEE Journal of Emerging and Selected Topics in Power Electronics



### C. Steady-State Responses

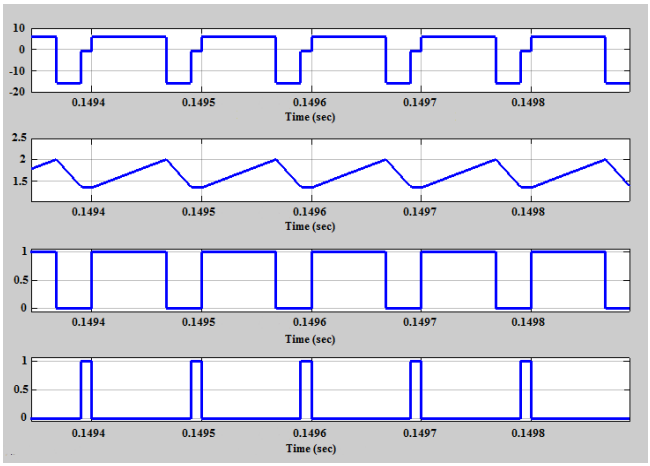


(a)

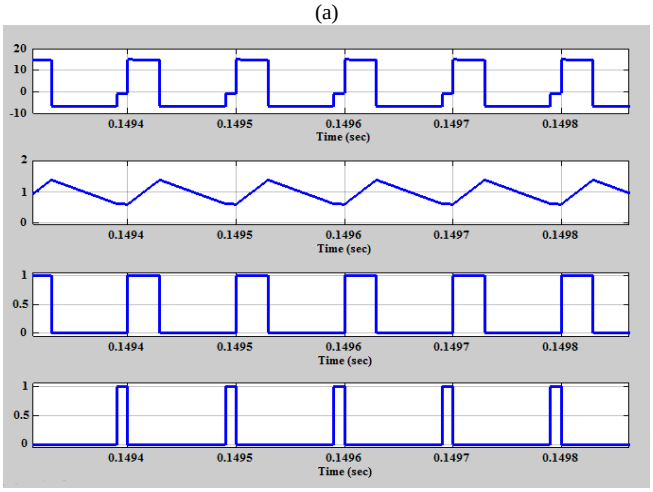


(b)

Fig.12. Steady-state waveforms of inductor voltage ($V_L$), inductor current ($i_L$), gate pulses for switches ($S_m$ & $S_f$) (a) Boosting mode (b) Bucking mode.

Extensive simulations are carried out in terms of load regulation and tracking performances (Fig.10&11) of both the converters with PSO based optimized Type-3 controller & "*K-factor*" based Type-3 controller. Fig.10(a)&(b) show the dynamic responses of output voltage when positive (+50%) and negative (-50%) sudden step disturbance is applied to the load resistance. It appears that the output voltage response of Tri-state Buck-Boost converter with PSO based optimized Type-3 controller is very fast and zero steady-state error. The tracking performances of both the converters are also observed (Fig.11(a)&(b)) by 20% positive & 20% negative step disturbances of the reference input voltage. From the Fig.11(a)&(b) output voltage of Tri-state Buck-Boost converter with PSO based optimized Type-3 controller is tracking the reference voltage quickly with zero overshoot & zero steady-state error. Fig.12(a)&(b) shows the steady-state simulation waveforms of inductor voltage ($V_L$), inductor current ($i_L$), and gate pulses for main and freewheeling switches ($S_m$ & $S_f$) of Tri-state Buck-Boost converter. From the Fig.12(a)&(b), when $S_m$ is on and $S_f$ is off, $V_L$= $V_S$ and $i_L$ is increasing. When both switches ($S_m$ & $S_f$) are off then $V_L$= (-$V_O$) and $i_L$ is decreasing. When $S_m$ is off and freewheeling switch $S_f$ is on then inductor voltage $V_L$ nearly equal to zero and inductor current $i_L$ is in freewheeling state.

### D. Comparison between Proposed and Existing RHP Zero Removal Method

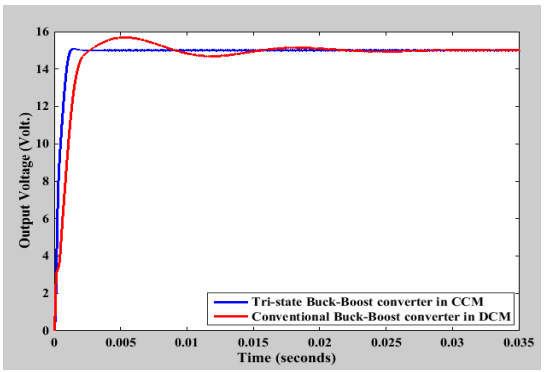


(a)

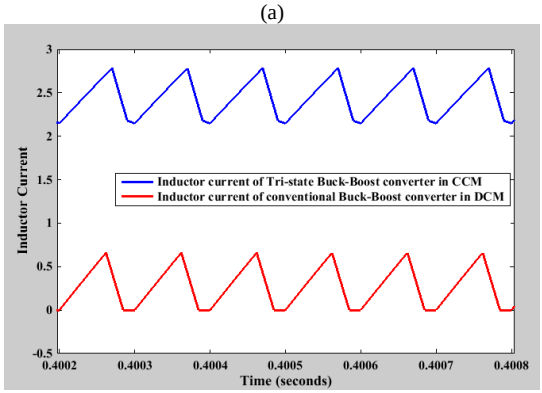


(b)

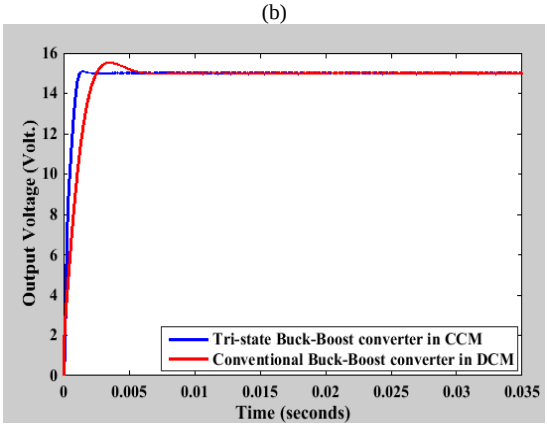


(c)

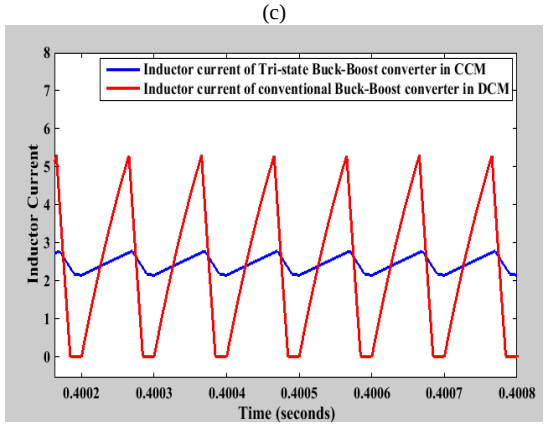


(d)

Fig.13. (a) Output voltage responses for case (i) and (b) Inductor currents waveform of conventional and Tri-state Buck-Boost converter for case (i), (c) Output voltage responses for case (ii) and (d) Inductor currents waveform of conventional and Tri-state Buck-Boost converter for case (ii).

There are some simple techniques presented in [5], which

This article has been accepted for publication in a future issue of this journal, but has not been fully edited. Content may change prior to final publication. Citation information: DOI 10.1109/JESTPE.2017.2724847, IEEE Journal of Emerging and Selected Topics in Power Electronics



can eliminate or reduce the effect of RHP zero for Boost or Buck-Boost converter. For example, by decreasing the value of inductor or by increasing the value of load resistance the Buck-Boost converter is forced to operate in DCM mode which will remove the effect of RHP zero. Both cases have been examined and the results have been compared with our proposed technique *i.e.* operating converter in Tri-state mode.

The DCM operation of conventional Buck-Boost converter is achieved by case (i) when load resistance is increased to 200 Ω & case (ii) the inductor value is decreased to 30 µH. Fig.13(a)&(c) shows the two closed-loop output voltage responses of Tri-state Buck-Boost converter & conventional Buck-Boost converter (operating under DCM) for the case (i) & (ii) respectively. It is seen that in both cases there is no effect of RHP zero, but Tri-state Buck-Boost converter exhibits better dynamic response with minimum overshoot, smaller rise & settling time with respect to Buck-Boost converter operating under DCM. The respective modes can be verified by observing the pattern of inductor currents shown in Fig.13(b)&(d) respectively. It is also noticed that the magnitude of ripple current in DCM operated Buck-Boost converter is much higher than Tri-state Buck-Boost converter.

Hence, it may be concluded that the proposed Tri-state Buck-Boost converter is superior to other RHP zero removal methods.

## VII. Experimental Results and Discussions

### A. Closed-loop Control Circuit and Experimental Setup

The closed-loop voltage-mode controlled Tri-state Buck-Boost converter with optimized Type-3 controller has been designed and fabricated in laboratory. The overall closed-loop control circuit diagram of Tri-state Buck-Boost converter is shown in Fig.14. The power circuit of the converter comprises a variable DC power source ($V_S$), two power MOSFETs (IRF450), two fast recovery diodes (MUR460), an energy storage inductor (275µH), an output filter capacitor (470µF) and a variable load resistance of 200 Ω, 40 Watts. An analog based control circuit is used for closed-loop voltage mode controlled of the proposed converter. In control circuit, NE555 timer based function generator is used which is generating sawtooth waveform at a frequency of 20 kHz. Two ICs (LM311) are the voltage comparator. IC1 (LM311) is comparing control voltage ($V_{con}$) with sawtooth waveform and generates PWM gate pulse for switch $S_m$. IC2 (LM311) is comparing freewheeling voltage ($V_f$) with sawtooth waveform and continuously generates PWM gate pulse for switch $S_f$. The freewheeling duration can be varied by varying the freewheeling voltage ($V_f$). Two opto-Isolators (MCT2E) are connected in the circuit for power and control circuit isolation. Two NE555 timers are connected as astable multivibrator mode to drive the gate of power MOSFETs. Overall hardware setup of Tri-state Buck-Boost converter is shown in Fig.15. The whole circuitry is fabricated in a PCB.

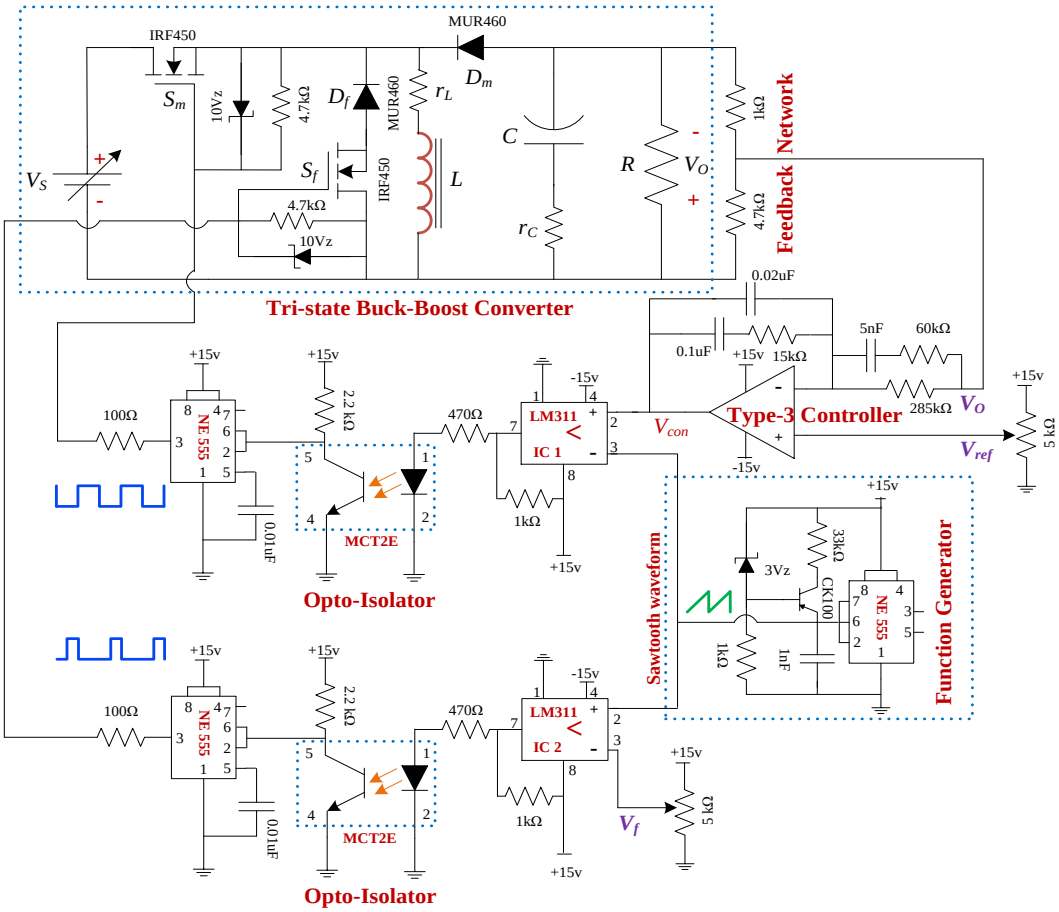


Fig.14. Complete closed-loop control circuit diagram of Tri-state Buck-Boost converter.

This article has been accepted for publication in a future issue of this journal, but has not been fully edited. Content may change prior to final publication. Citation information: DOI 10.1109/JESTPE.2017.2724847, IEEE Journal of Emerging and Selected Topics in Power Electronics



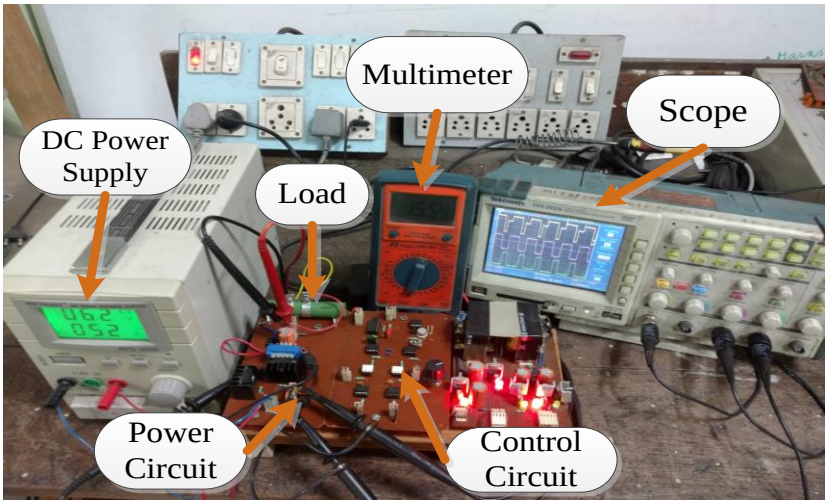


Fig.15. Hardware setup of Tri-state Buck-Boost converter.

## B. *Experimental Results*

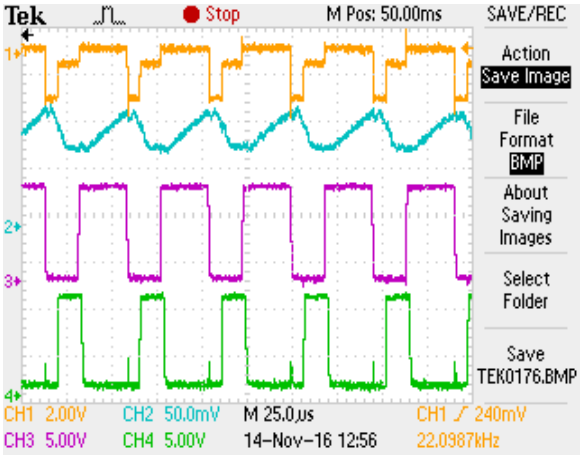


(a)

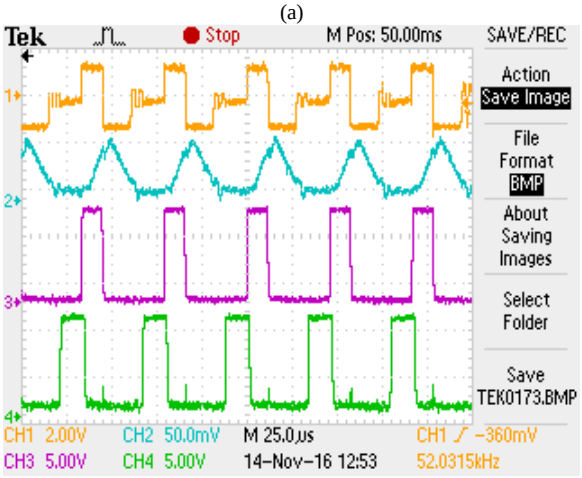


(b)

Fig.16. Experimental steady-state waveforms of Tri-state Buck-Boost converter in (a) Boosting mode & (b) Bucking mode, Ch-1: inductor voltage, Ch-2: inductor current, Ch-3: gate pulse for $S_m$, Ch-4: gate pulse for $S_f$.

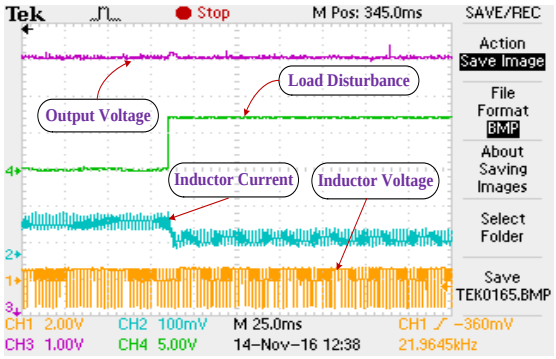


(a)

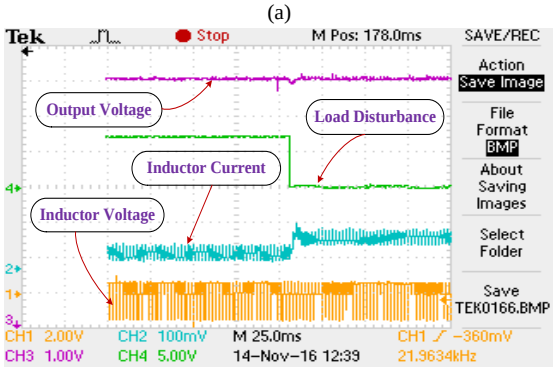


(b)

Fig.17. Dynamic response of output voltage of Tri-state Buck-Boost converter with (a) 50 % step increased & (b) 50 % step decreased of load resistance in Boosting mode; Ch-1: inductor voltage, Ch-2: inductor current, Ch-3: output voltage, Ch-4: load disturbance.

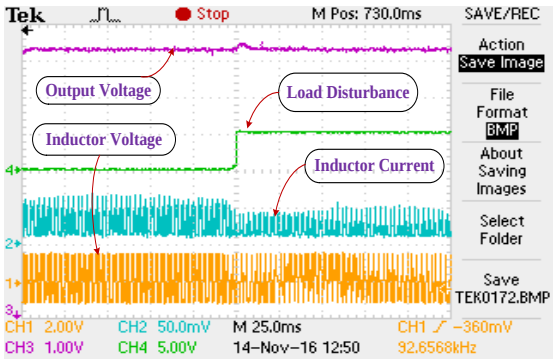


(a)

This article has been accepted for publication in a future issue of this journal, but has not been fully edited. Content may change prior to final publication. Citation information: DOI 10.1109/JESTPE.2017.2724847, IEEE Journal of Emerging and Selected Topics in Power Electronics



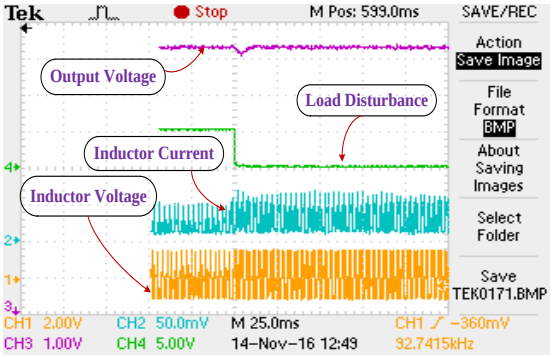


(b)

Fig.18. Dynamic response of output voltage of Tri-state Buck-Boost converter with (a) 50 % step increased & (b) 50 % step decreased of load resistance in Bucking mode; Ch-1: inductor voltage, Ch-2: inductor current, Ch-3: output voltage, Ch-4: load disturbance.

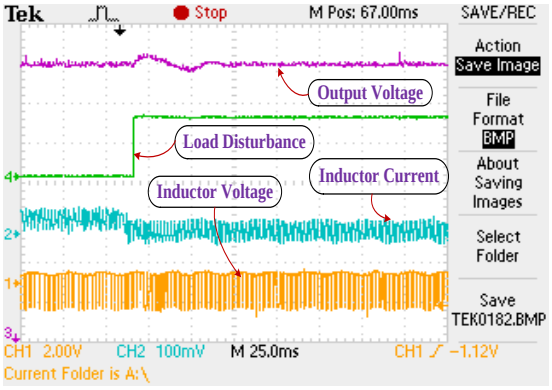


(a)

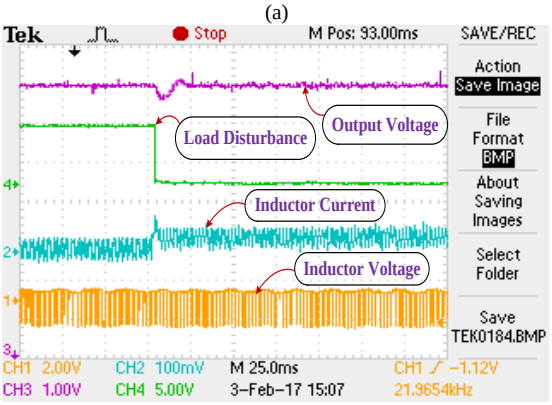


(b)

Fig.19. Dynamic response of output voltage of conventional Buck-Boost converter with (a) 50 % step increased & (b) 50 % step decreased of load resistance in Boosting mode; Ch-1: inductor voltage, Ch-2: inductor current, Ch-3: output voltage, Ch-4: load disturbance.

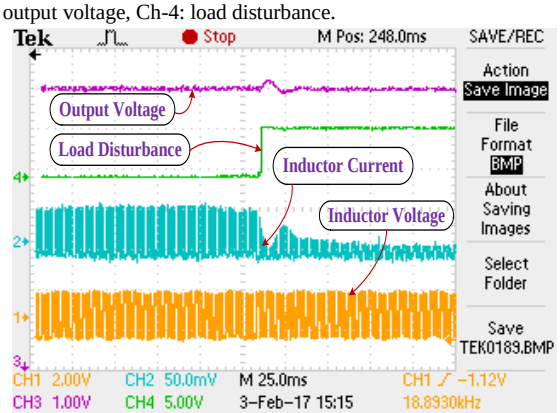


(a)

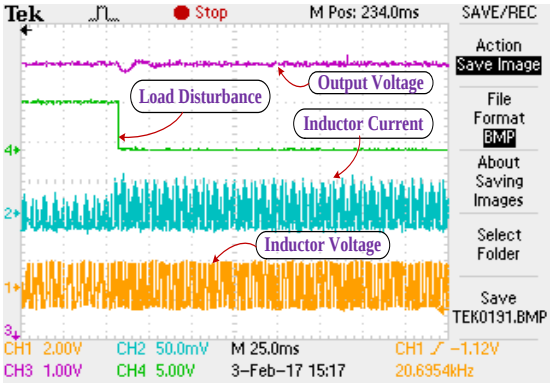


(b)

Fig.20. Dynamic response of output voltage of conventional Buck-Boost converter with (a) 50 % step increased & (b) 50 % step decreased of load resistance in Bucking mode; Ch-1: inductor voltage, Ch-2: inductor current, Ch-3: output voltage, Ch-4: load disturbance.

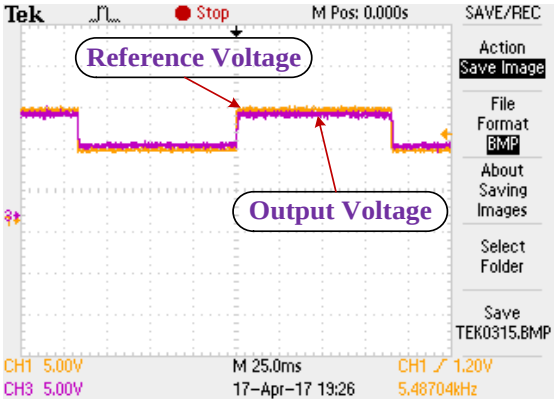


(a)

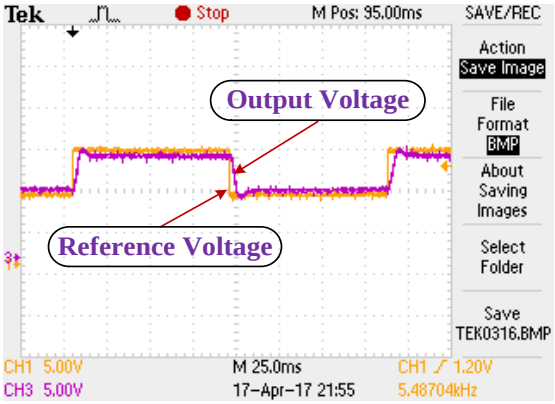


(b)

Fig.21. Output voltage response against square wave step disturbance applied to the reference voltage (a) Tri-state Buck-Boost converter (b) Conventional Buck-Boost converter; Ch-1: Reference voltage, Ch-3: Output voltage.

It is evident from simulation results (Fig.9 to Fig.11) that the proposed Tri-state Buck-Boost converter with PSO based optimized Type-3 controller has been performed better compared to conventional Buck-Boost converter. Accordingly PSO based optimized Type-3 controller has also been utilized for practical closed-loop control of the proposed Tri-state Buck-Boost converter. Experimental steady-state waveforms of inductor voltage ($V_L$), inductor current ($i_L$), gate pulses for main ($S_m$) & freewheeling ($S_f$) switches of the proposed converter are shown in Fig.16(a)&(b). A FLUKE made current probe (scale 100mV=1A) is used to measure the inductor current. Fig.17 to Fig.20 show the dynamic responses

This article has been accepted for publication in a future issue of this journal, but has not been fully edited. Content may change prior to final publication. Citation information: DOI 10.1109/JESTPE.2017.2724847, IEEE Journal of Emerging and Selected Topics in Power Electronics



of output voltage of Tri-state Buck-Boost converter and conventional Buck-Boost converter with PSO based optimized Type-3 controller for positive & negative step disturbance of load resistance (50%). The experimental output voltage responses of Tri-state Buck-Boost converter and conventional Buck-Boost converter have been observed with the square wave step-input change of reference voltage ($V_{ref}$) and are shown in Fig.21. It is observed that the proposed Tri-state Buck-Boost converter shows better transient and steady-state performances compared to conventional Buck-Boost converter in all cases.

## VIII. Conclusion

In this paper, modeling, design and practical implementation of Tri-state Buck-Boost converter with PSO based optimized Type-3 controller has been presented. The small-signal modeling of Tri-state Buck-Boost converter has been developed by using state-space averaging technique to find the control-to-output transfer function. It can be concluded that there is no RHP zero in control-to-output transfer function of the proposed converter. A Type-3 controller has been designed by using "*K-factor*" approach and its transfer function has been optimized by using PSO based optimization technique to improve the transient & steady-state performances. A simple analog control circuit has been designed to reduce the overall cost and circuit complexity. Simulation and experimental results of the proposed Tri-state Buck-Boost converter and conventional Buck-Boost converter have been presented and a comparative study has been done.

It can be identified that the Tri-state Buck-Boost converter with optimized Type-3 controller exhibits the best closed-loop performance with largest margin of stability and highest system bandwidth. So, Tri-state Buck-Boost converter with optimized Type-3 controller may be implemented for designing the DC-DC switching converter to enhance the overall closed-loop performance and stability of the power supplies. The proposed converter can be used for drive applications, electric vehicles, photovoltaic system and any fast-response SMPS to provide power for new generation DSP/Microprocessor systems, electronic goods and gadgets, telecom power supplies, critical medical equipment/ instruments etc. However, the efficiency of the proposed Tri-state Buck-Boost converter is comparatively less than that of the conventional Buck-Boost converter due to the losses incurred in the additional circuit elements and also the cost of proposed converter will be little higher compared to conventional one.

## References


[1] R. W. Erickson, and D. Maksimovic, *Fundamentals of Power Electronics*, Berlin, Germany, Springer, 2007.

[2] K. Ogata, *Modern Control Engineering*, India, Pearson Education, 2010.

[3] S. Kapat, A. Patra, and S. Banerjee, "A Current-Controlled Tristate Boost Converter With Improved Performance Through RHP Zero Elimination," *IEEE Transactions on Power Electron*ics, vol. 24, no. 3, pp. 776-786, Mar. 2009.

[4] K. Viswanathan, R. Oruganti, and D. Srinivasan, "Dual-Mode Control of Tri-State Boost Converter for Improved Performance" *IEEE Transactions on Power Electron*ics, vol. 20, no. 4, pp. 790-797, Jul. 2005.

[5] W. C. Wu, R. M. Bass, and J. R. Yeargan, "Eliminating the Effects of the Right-Half Plane Zero in Fixed Frequency Boost Converters," in *Proc. IEEE29th Annual Power Electronics Specialists Conference (PESC 1998)*, vol. 1, pp. 362-366, 1998.

[6] D. M. Sable, B. H. Cho, and R. B. Ridley, "Use of Leading-Edge Modulation to Transform Boost and Flyback Converters into Minimum-Phase-Zero Systems," *IEEE Transactions on Power Electron*ics, vo1. 6, no. 4, pp. 704-711, Oct. 1991.

[7] K. Viswanathan, R. Oruganti, and D. Srinivasan, "A Novel Tri-State Boost Converter with Fast Dynamics," *IEEE Transactions on Power Electron*ics, vol. 17, no. 5, pp. 677-683, Sep. 2002.

[8] K. Viswanathan, "Dynamic Performance Improvement in Boost and Buck-Boost Derived Power Electronic Converters," Doctoral dissertation, 2005.

[9] S. Sarkar, A. Ghosh, and S. Banerjee, "Design and Implementation of Type-III Controller in Tri State Boost Converter," in *proc. 12th IEEE India Council International Conference (INDICON 2015)*, pp. 1-6, New Delhi, India, 2015.

[10] N. Mohan, T. M. Undeland, and W. P. Robbins, *Power Electronics*, New York, Wiley, 2003.

[11] E. Rogers, "Understanding Buck-Boost Power Stages in Switch Mode Power Supplies," *Texas Instruments*, Application Report, SLVA059A, pp. 1-32, Nov. 2002.

[12] B. Sahu, and G. A. Rincon-Mora, "A Low Voltage Dynamic Non inverting Synchronous Buck-Boost Converter for Portable Applications," *IEEE Transactions on Power Electron*ics, vol. 19, no. 2, pp. 443-452, Mar. 2004.

[13] M. He, F. Zhang, J. Xu, P. Yang, and T. Yan, "High-efficiency two-switch tri-state buck-boost power factor correction converter with fast dynamic response and low-inductor current ripple," *IET Power Electronics*, vol. 6, no. 8, pp. 1544-1554, 2013.

[14] A. Ghosh, S. Banerjee, M. K. Sarkar, and P. Dutta, "Design and Implementation of Type-II and Type-III Controller for DC-DC Switched-Mode Boost Converter by using K-Factor Approach and Optimization Techniques," *IET Power Electronics*, vol. 9, no. 5, pp. 938-950, 2016.

[15] H. D. Venable, "The K-Factor: A New Mathematical Tool for Stability Analysis and Synthesis," in *Proc. Powercon*, San Diego, USA, 1983.

[16] A. Ghosh, and S. Banerjee, "Design of Type-III Controller for DC-DC Switch Mode Boost Converter," in *proc. IEEE 6th Power India International Conference (PIICON 2014)*, pp. 1-6, New Delhi, India, Dec. 2014.

[17] A. Ghosh, and S. Banerjee, "Design and implementation of Type-II compensator in DC-DC switch-mode step-up power supply," in *proc. IEEE 3rd International Conference on Computer, Communication, Control and Information Technology (C3IT 2015)*, pp. 1-5, 2015.

[18] S. Banerjee, A. Ghosh, and N. Rana, "Design and Fabrication of Closed Loop Two-Phase Interleaved Boost Converter with Type-III Controller," in *proc. 42nd Annual Conference of the IEEE Industrial Electronics Society (IECON 2016)*, pp. 3331-3336, 2016.

[19] J. Kennedy, and R. C. Eberhart, "Particle Swarm Optimization," in *proc. IEEE International Conference on Neural Network*, vol. 4, pp. 1942-1948, 1995.

[20] J. Kennedy, "Particle Swarm Optimization," *Encyclopedia of Machine Learning*, pp. 760-766, 2010.

[21] X. Li, "A Particle Swarm Optimization and Immune Theory-Based Algorithm for Structure Learning of Bayesian Networks," *International Journal of Database Theory and Application*, vol. 3, no. 2, 2010.

[22] M. Clerc, "Particle Swarm Optimization," *John Wiley and Sons*, 2010.

[23] Y. A. I. Mohamed, and E. F. E. Saadany, "Hybrid Variable-Structure Control With Evolutionary Optimum-Tuning Algorithm for Fast Grid-Voltage Regulation Using Inverter-Based Distributed Generation," *IEEE Transactions on Power Electron*ics, vol. 23, no. 3, pp. 1334-1341, May. 2008.

[24] C. Yang, S. XIE, L. Mao, and Z. Zhang, "Efficiency Improvement on Two-Switch Buck-Boost Converter with Coupled Inductor for High-Voltage Applications," *IET Power Electronics*, vol. 7, no. 11, pp. 2846-2856, 2014.

[25] M. Veerachary, and A. R. Saxena, "Optimized Power Stage Design of Low Source Current Ripple Fourth-Order Boost DC-DC Converter: A PSO Approach,"*IEEE Transactions on Industrial Electronics*, vol. 62, no. 3, pp. 1491-1502, Mar. 2015.

[26] A. Ghosh, S. Banerjee, and P. Dutta, "Gravitational Search Algorithm based optimal Type-II controller for DC-DC Boost Converter," in *proc. Michael Faraday IET International Summit (MFIIS 2015)*, pp. 374-379, India, 2015.

[27] Z. Fang, T. Cai, S. Duan, and C. Chen, "Optimal Design Methodology for LLC Resonant Converter in Battery Charging Application Based on Time-Weighted Average Efficiency," *IEEE Transactions on Power Electron*ics, vol. 30, no. 10, pp. 5469-5483, Oct. 2015.

[28] A. Ghosh, and S. Banerjee, "Control of Switched-Mode Boost Converter by using Classical and Optimized Type Controllers," *Journal of Control Engineering and Applied Informatics*, vol. 17, no. 4, pp. 114-125, 2015.

[29] Y. Lu, H. Wu, K. Sun, and Y. Xing, "A Family of Isolated Buck-Boost Converters Based on Semiactive Rectifiers for High-Output Voltage Applications" *IEEE Transactions on Power Electron*ics, vol. 31, no. 9, pp. 6327-6340, Sep. 2016.

[30] A. Darwish, A. M. Massoud, D. Holliday, S. Ahmed, and B. W. Williams, "Single-Stage Three-Phase Differential-Mode Buck-Boost Inverters with Continuous Input Current for PV Applications," *IEEE Transactions on Power Electron*ics, vol. 31, no. 12, pp. 8218-8236, Dec. 2016.

[31] H. Wu, T. Mu, H. Ge, and Y. Xing, "Full-range soft-switching-isolated buck-boost converters with integrated interleaved boost converter and phase-shifted control," *IEEE Transactions on Power Electron*ics, vol. 31, no. 2, pp. 987-999, Feb. 2016.

[32] R. Ren, B. Liu, E. A. Jones, F. F. Wang, Z. Zhang, and D. Costinett,"Capacitor-clamped, three-level GaN-based DC–DC Converter With Dual Voltage Outputs for Battery Charger Applications," *IEEE Journal of Emerging and Selected Topics in Power Electronics*, vol. 4, no. 3, pp. 841-853, Sep. 2016.

[33] Z. Guo, K. Sun, and L. Zhang, "Analysis and Evaluation of Dual Half-Bridge Cascaded Three-Level DC-DC Converter for Reducing Circulating Current Loss," *IEEE Journal of Emerging and Selected Topics in Power Electronics*, vol. 5, no. 1, pp. 351-362, Mar. 2017.

[34] S. Banerjee, A. Ghosh, and N. Rana, "An Improved Interleaved Boost Converter with PSO Based Optimal Type-III Controller," *IEEE Journal of Emerging and Selected Topics in Power Electronics*, vol. 5, no. 1, pp. 323-337, Mar. 2017.

[35] D. Vinnikov, A. Chub, R. Kosenko, J. Zakis, and E. Liivik, "Comparison of Performance of Phase-Shift and Asymmetrical Pulsewidth Modulation Techniques for the Novel Galvanically Isolated Buck-Boost DC-DC Converter for Photovoltaic Applications," *IEEE Journal of Emerging and Selected Topics in Power Electronics*, vol. 5, no. 2, pp. 624-637, Jun. 2017.

[36] T. Kobaku, S. C. Patwardhan, and V. Agarwal, "Experimental Evaluation of Internal Model Control Scheme on a DC-DC Boost Converter Exhibiting Nonminimum Phase Behavior," *IEEE Transactions on Power Electron*ics, vol. 32, no. 11, pp. 8880-8891, Nov. 2017.

**Niraj Rana** (S'17) received the B.Tech degree in Electrical Engineering from Government College of Engineering Keonjhar, Odisha, India in 2013 and M.Tech degree in Power Electronics and Machine Drives from National Institute of Technology Durgapur, India in 2016.

Currently, he is pursuing the Ph.D degree in the Department of Electrical Engineering, National Institute of Technology Durgapur, India. His fields of interest include power electronics converters, applications of power electronics converters in renewable energy systems, maglev train and magnetic levitation systems, wireless power transfer technology and robotics etc.

**Arnab Ghosh** (S'13–M'16) was born in Kalyani, West Bengal, India, in 1988. He received his B.Tech, M.Tech degree in Electrical Engineering in the year of 2010 & 2012 respectively from West Bengal University of Technology. He has completed his Ph.D in Electrical Engineering from National Institute of Technology Durgapur in the year 2017.

He is currently working as an Assistant Professor in Department of Electrical Engineering at Dr. B. C. Roy Engineering College, Durgapur, India. He has published a numbers of research papers in National/International Journals and Conference Records. His research interest includes control of switch-mode converters, non-linear dynamics of converters, machine drives etc.

**Subrata Banerjee** (M'04–SM'15) received his Ph.D in Electrical Engineering from Indian Institute of Technology, Kharagpur in the year 2005.

He is presently working as Professor in Electrical Engineering at National Institute of Technology, Durgapur, India. He has published a numbers of research papers in National/International Journals and Conference Records. His area of interest includes Electromagnetic Levitation, Active Magnetic Bearing, Controller Design, Intelligent Control, Optimization Techniques, Control of Switch-mode converters and non-linear dynamics of converters etc. He is a Fellow of Institute of Engineers (India), life member of Systems Society of India, and senior member of IEEE (USA). He has successfully completed some research and consultancy projects including one major from DST, Govt. of India. His Biographical inclusion is in Marquis Who's Who 2007 and IBC FOREMOST Engineers of world-2008. Prof. Banerjee has received few academic awards including 4 no. of Best papers, TATA RAO Prize in his credit. He has filed one Indian Patent in 2013. Prof. Banerjee is acting as regular reviewer of IEEE Transaction on PE, IEEE Transaction on IE, Electrical Power Components and Systems etc.